

PAPER • OPEN ACCESS

Hydrophobicity of laser-textured soda-lime glass

To cite this article: K. A. Nur Najwa *et al* 2024 *J. Phys.: Conf. Ser.* **2688** 012021

View the [article online](#) for updates and enhancements.



PRIME
PACIFIC RIM MEETING
ON ELECTROCHEMICAL
AND SOLID STATE SCIENCE

HONOLULU, HI
Oct 6–11, 2024

Abstract submission deadline:
April 12, 2024

Learn more and submit!

Joint Meeting of

The Electrochemical Society
•
The Electrochemical Society of Japan
•
Korea Electrochemical Society

Hydrophobicity of laser-textured soda-lime glass

K. A. Nur Najwa¹, M. Hilmi¹, S. N. Aqida^{1,2,*}, I. Ismail^{2,3}

¹Faculty of Mechanical and Automotive Engineering Technology,
Universiti Malaysia Pahang Al-Sultan Abdullah, 26600 Pekan, Pahang, Malaysia,
²Automotive Engineering Centre, Universiti Malaysia Pahang Al-Sultan Abdullah,
26600 Pekan, Pahang, Malaysia

³Faculty of Manufacturing and Mechatronic Engineering Technology,
Universiti Malaysia Pahang Al-Sultan Abdullah, 26600 Pekan, Pahang, Malaysia,

*Corresponding Email: aqida@ump.edu.my

Abstract. This paper studies the effect of the modified soda-lime glass surface that reduces water adhesion and raises the water contact angle by modifying the laser processing parameter. The study looked at how these variables affected the water contact angle and surface morphology. The characterization was performed using an inverted metallurgical microscope for surface morphology, and a sessile drop test setup for water contact angle measurement and bricklayer pattern with two different hatch spacings of 0.3 and 0.5 mm was used. The results revealed that the highest water contact angle achieved after surface modification for 0.3 mm was 98.97° at 1000 mm/min and 1.0 W while for 0.5 mm at 93.01°, at 600 mm/min and 1.2 W, improved its hydrophobicity from untextured glass 32.35°. Both sample patterns with 0.3 and 0.5 mm show no defect and all samples seem to have a mark from laser texturing with an increase in power, the laser mark on the surface becomes wider and the large gap between the line becomes more distinct. These findings are significant for designing hydrophobic glass surfaces using laser texturing.

Keywords: Hydrophobic, Laser texturing, Sessile drop, Contact angle

1. Introduction

Laser machining is widely used in industry to cut, clean, and change the surface of glass. Laser machining is a revolutionary and contactless kind of machining process, and it is used commonly in engineering materials due to its accuracy and efficacy for patterning on a variety of substrates made of different materials [1]. Recently, one of the methods is laser surface texturing (LST), laser machining processes are recognized as a special method of surface treatment [2]. One of the most effective methods for modifying and controlling crucial surface functions, such as surface wettability [3][4][5], reflectivity, anti-icing properties [5][6], corrosion resistance [5][7], etc. is laser-based surface texturing. In contrast to other methods of surface modification like machining and sandblasting, laser surface processing produces a consistent surface structure directly. Contrary to coating, laser processing does not suffer from a problem with surface adhesion to mass material. Previous study shows that the innovation of laser was used to enhance a material's wettability, corrosiveness, wear, and mechanical properties. The laser material processing efficacy to produce higher surface characteristics has been the subject of numerous investigations. Using the right laser processing parameters will successfully alter a material's wetting qualities [8].

Water repellency, often known as hydrophobicity, is one of the most significant surface qualities of materials. Surfaces of materials are classified into four stages, superhydrophilic, hydrophilic, hydrophobic, and superhydrophobic depending on their wettability. The classifications are made based on their contact angle (CA) the solid surface is greater than 90° but less than 150°, and it is hydrophobic. Surfaces are referred to as superhydrophobic when the CA value is between 150° and 180°. The representatives that impact the CA are surface energy, roughness, cleanliness, and surface preparation method [9].



Additionally, metals that consist of (copper, aluminum, and titanium), while ceramics consist of (glass and sapphire), polymers, and silicon are the usage by a range of substances to produce superhydrophobic surfaces [10]. Glass stands out among these materials for a variety of applications that require great optical clarity, chemical stability, heat resistance, hardness, or biological suitability [11]. A wider range of applications for these materials has been made possible by functionalizing glasses by surface modification, which has revealed appealing properties for high-value products [11]. Surface modifications, which involve altering the outermost layer, are a commonly employed technique for imparting advantageous properties. Materials subjected to surface treatment can be easily found and the process can be carried out through various physical or chemical means. Physical methods are used during fabrication to modify the surface, enabling the attainment of superhydrophobic and omni-phobic surfaces by introducing roughness and altering surface wettability [12].

Prior investigations about the hydrophobicity of soda-lime-silica glass surfaces have demonstrated that the surface transforms from being hydrophilic to becoming hydrophobic, with CA value from lower 20° to close to 125° , employing a salinization solution in conjunction with femtosecond laser irradiation for chemical treatment [13]. Another important element in determining CA is laser power. Scan speed has little effect on the depth of the channel; the only determinant is channel width. Because of the scan's speed, the laser frequency results are also the same. Although the depth of the channel grows with frequency, neither does the frequency affect the hydrophobicity. After Dongre, et al., droplet's test, the laser's power and scan speed greatly affected the CA identified [14].

In consequence, this study explores recent studies on a hydrophobic surface on soda-lime glass produced using the process of laser textured to determine the effect of laser parameters on surface morphology and contact angle of modified glass surface. The CA was measured using the sessile drop test on untextured and textured glass with minimal glass cracking. The hydrophobicity of textured patterns for 0.3 and 0.5 mm hatch spacing was discussed in correlation to the laser parameters.

2. Experimental setup

An Atomstack A20 Pro Laser diode laser machine with continuous wave processing mode and a laser wavelength of 445 nm was used in the surface text of the resurface surface. The laser texture was operated using the LightBurn software and the setup is shown in Figure 1.

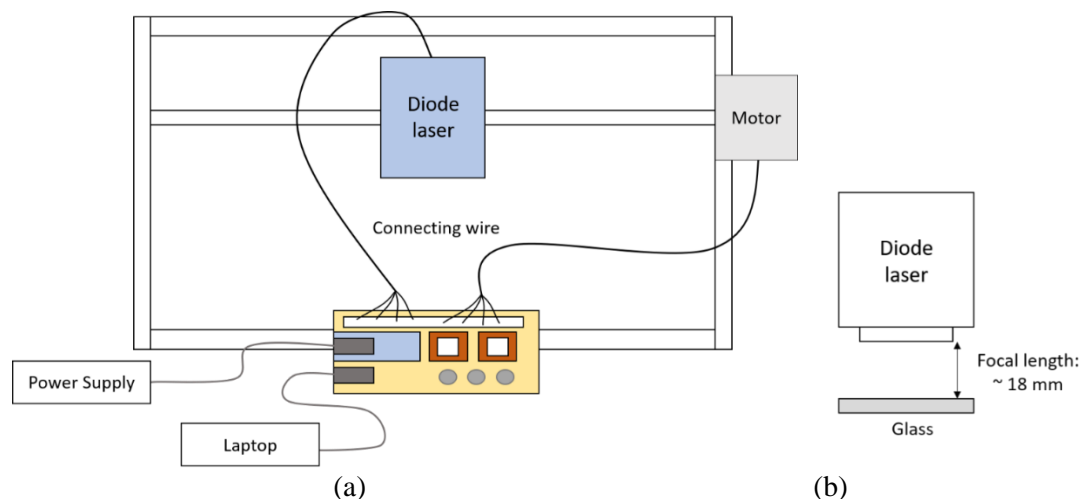


Figure 1. Schematic diagram (a) laser texturing of glass set-up and, (b) focal length distance

The material used in this study is soda-lime glass, with a thickness of 1.0 mm and a dimension of 76×26 mm (manufactured by HmbG), with the chemistry listed in Table 1. The glass surface was textured with bricklayer patterns as shown in Figure 2 where two different hatch spacing sizes were made; the first one was 0.5 mm spacing for each square and the other one was 0.3 mm, while the fabrication area was

5×5 mm². All samples were then allowed to experiment after laser textured, and the impact of laser power and scanning speed on hydrophobicity was recorded. Process parameter is summarized in Table 2, this is crucial to the experiment since it shows different responses in the result for the contact angle measurement and morphology. The line distance is a factor in investigating its effect on glass surface hydrophobicity.

Table 1. Chemical composition of soda-lime glass

Oxides	SiO ₂	Na ₂ O	K ₂ O	CaO	MgO	Al ₂ O ₃	Fe ₂ O ₃	SO ₃
wt.%	72.20	14.30	1.20	6.40	4.30	1.20	0.03	0.30

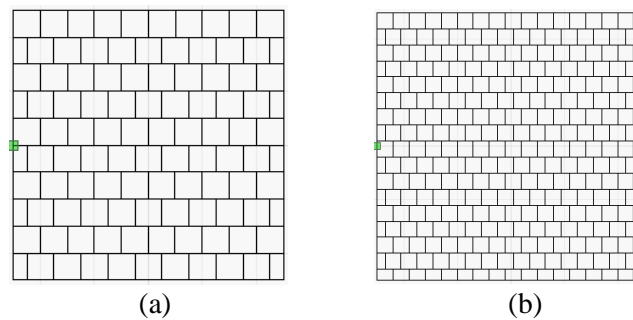


Figure 2. Bricklayer pattern design; (a) 0.5 mm spacing, (b) 0.3 mm spacing

Table 2. Design of experiment for laser texture of glass surface

Standard order	Speed (mm/min)	Power (Watts)
1	600	1.0
2	600	1.2
3	600	1.4
4	800	1.0
5	800	1.2
6	800	1.4
7	1000	1.0
8	1000	1.2
9	1000	1.4

The CA of the patterned surface of the glass was measured using the sessile drop technique setup. The reagent used in this experiment was type II reagent water (distilled water) by ASTM D1193. The measured CA of water on the samples was conducted according to the practice of ASTM D7334 [15] using a Hamilton microliter syringe. A 3.3 μl volume of droplet was deposited on the glass surface and was measured quickly, within 30 seconds of the drop being deposited, to prevent angle variations as the water evaporated [15]. A microscope that magnifies the contact area according to the Test Method

ASTM D5725 [16], with a maximum magnification of $100\times$ is connected to a laptop for capturing images of the droplet. The images were captured and converted to grayscale mode and then transferred to ImageJ software. Further analysis of CA in ImageJ software was carried out using the Low Bond Axisymmetric Drop Shape Analysis (LB-ADSA) plugin.

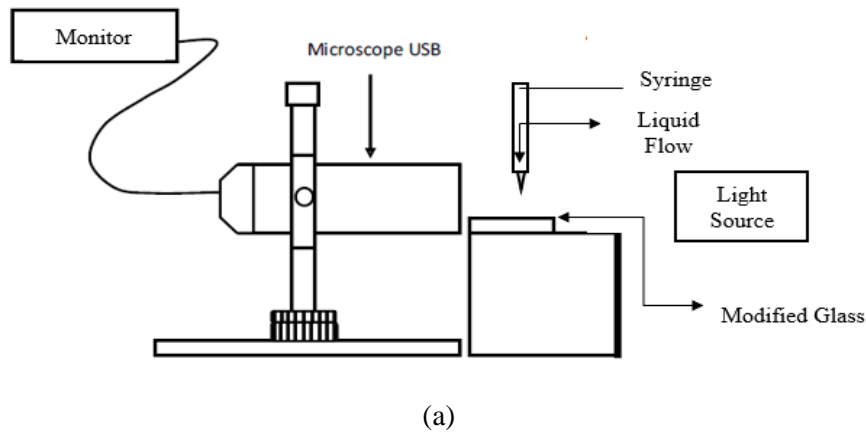


Figure 3. (a) A schematic setup of the sessile drop test

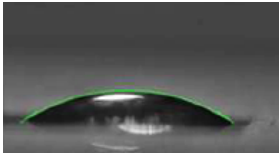
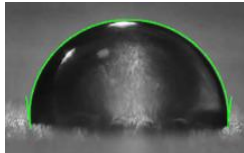
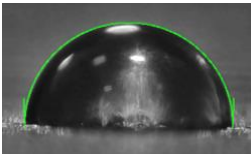
The surface morphology to analyze the shape of irregularities on a micro-structured surface, micrographs are captured using an inverted metallurgical microscope, specifically the Meiji Techno IM7200 Inverted Trinocular Metallurgical Microscope with a 6V, 30W Halogen light source. The microscope is equipped with infinity-corrected Planachromat objectives at $5\times$, $10\times$, $20\times$ and $50\times$ magnifications, providing diverse levels of magnification for detailed observation. It also features a front-mounted camera that allows for optional adapters. By connecting the microscope to a computer, digital micrographs can be obtained and saved using the mounted camera.

3. Results and discussion

3.1 Water Contact Angle

Laser-textured glass surface exhibits different CA at different laser power and scanning speed. The resulting CA can be seen in Table 3 where the unmodified glass surface has hydrophilic properties with a 32.25° CA. After textures, the CA for 0.3 mm and 0.5 mm hatch spacing increased up to 98.97° and 93.01° respectively. Overall, the CA increases after laser surface textures, where the hydrophilicity of the glass surface is reduced, approaching hydrophobic. The hatch spacing in the pattern had an impact on the CA in addition to laser parameters.

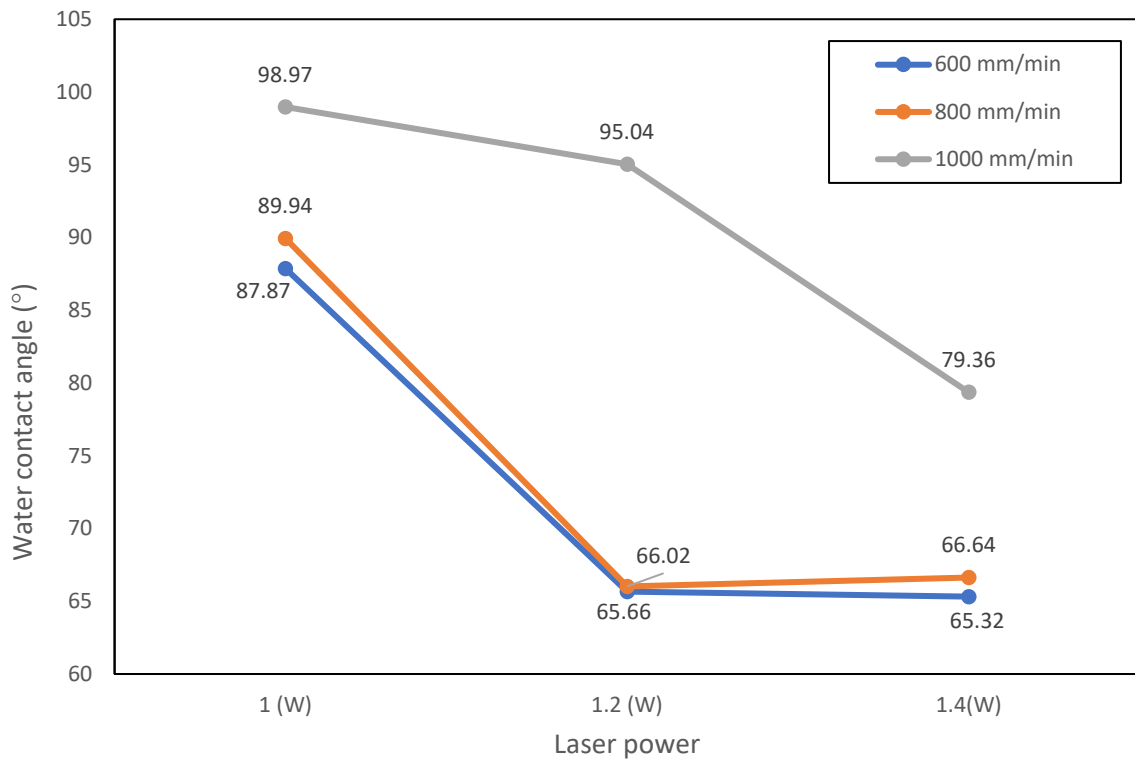
Table 3. The highest water contact angle for each pattern

	Untextured glass	0.3 mm brick layer pattern	0.5 mm brick layer pattern
WCA ($^\circ$)	 32.35 $^\circ$	 98.97 $^\circ$	 93.01 $^\circ$

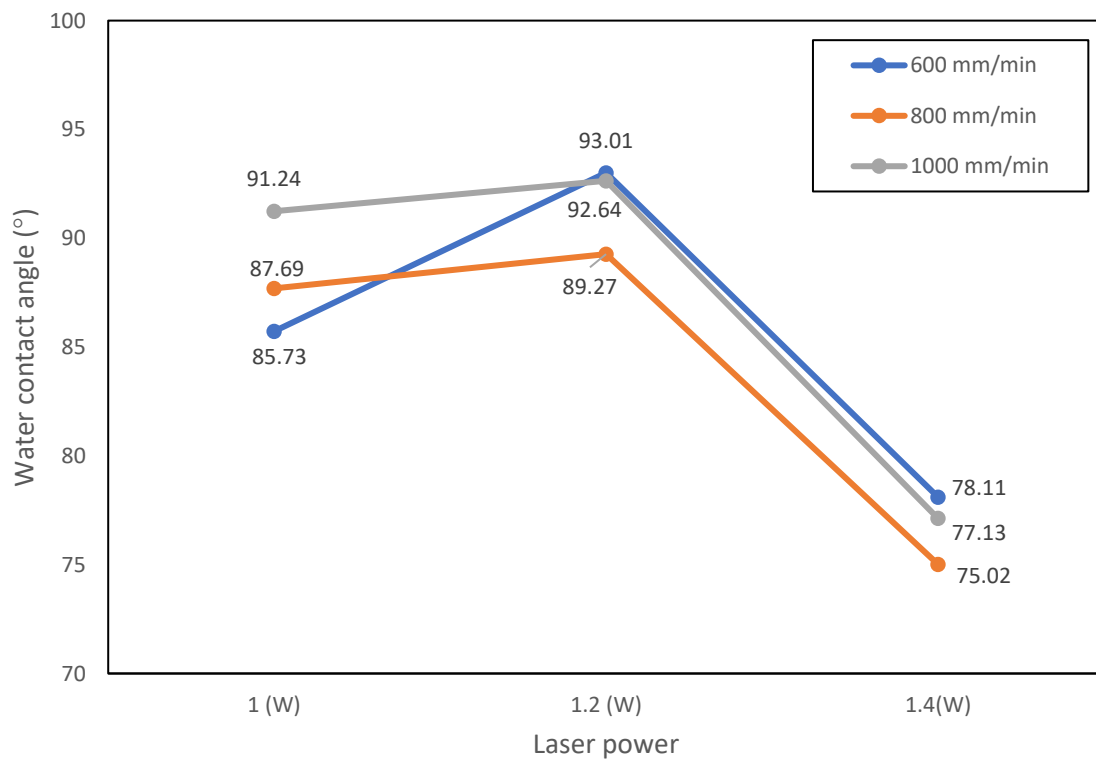
In this experiment, the laser power was changed from 1.0 to 1.4 W, and from 600 to 1000 mm/min scan speed was used. Sample 7 comes with 1 W and 1000 mm/min that exhibit the maximum CA for the 0.3 mm brick layer pattern at 98.97°. Sample 3 had the lowest CA, which was 65.32° with a 1.4W laser and a 600 mm/min scanning speed. Lower laser power and faster scan speeds tend to produce higher CA, according to measurements of the CA against the parameter. In particular, the trend indicates a reduction in CA as laser power rises. Dongre et al. claim that the scan speed impacts the CA most. In conjunction with the scan speed, the CA also increases. The channel width increases together with the scan speed, but only up to a scan speed of 800 mm/sec. The channel width narrows after that [14]. In comparison to earlier studies, the CA is also growing linearly as laser power rises. The increase in CA does not continue throughout the range. The graph's slope has changed somewhat, and the channel's width and depth have increased. The CA has also increased to 157°. Between 6 W and 12 W of laser power were employed; anything above that causes the material to oxidize and lose its texture [14].

Sample 2 with 1.2 W and 600 mm/min has the maximum CA for the 0.5 mm brick layer pattern at 93.01°. Sample 6 with 1.4 W and 800 mm/min, showed the lowest CA, which is 75.02°. The CA measurements against the parameter reveal that lower laser power and higher scan speed tend to result in higher CA. Different from the sample 0.3 mm before, the CA for the sample 0.5 mm pattern has a different outcome. At a laser power of 1.2W in particular, the trend indicates an increase in CA, particularly at scanning speeds of 600 mm/min and 1000 mm/min. The CA is substantially higher with a laser power of 1.2 W than it is at 1.0 W. However, given that a human error disrupted the sessile drop test for the glass, it is possible. This revealed variations in laser power intensity and scan speed did not significantly affect the CA measurement.

In contrast, high-energy laser therapy produced more hydrophilic surfaces, according to research, whereas low-energy laser treatment made surfaces more hydrophobic. Additionally, the impact of laser power on wettability was more prominent compared to the scan speed [17]. As laser power increases, the CA decreases compared to the as-received material as the work of adhesion energy increases when laser power density increases [8].



(a) 0.3 mm pattern



(b) 0.5 mm pattern

Figure 4. Interaction plot for water contact angle measurement for (a) 0.3 mm, and (b) 0.5 mm spacing pattern

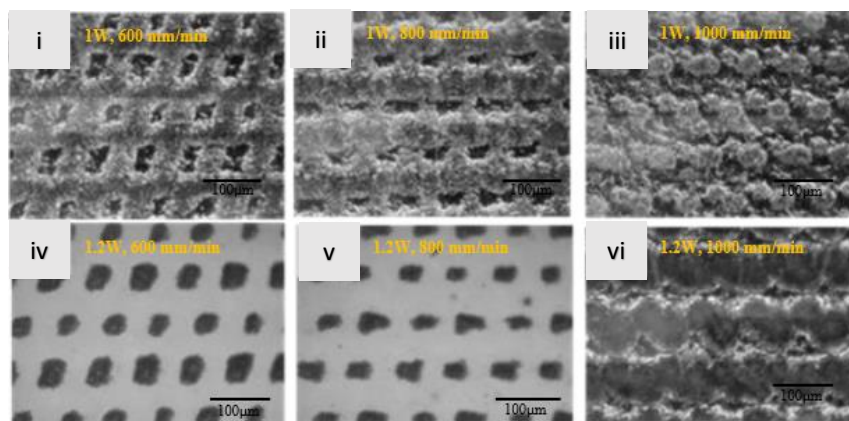
Figure 4(a) shows an interaction plot for a 0.3mm and Figure 4(b) shows an interaction plot for a 0.5mm spacing pattern, illustrating the relationship between laser power, scanning speed, and the highest water contact angle achieved for each sample. The plot displays a line graph for the scanning speed parameter while varying the laser power. For 0.3 mm all the lines representing different scanning speeds are parallel to each other while for 0.5 mm they are not parallel to each other. This interaction effect suggests that the impact of laser power on the CA depends on the specific value of scanning speed and significantly influences the resulting CA value. The greatest measured CA value for each laser power level is shown in Figure 4(a) at 1000 mm/min scan speed, and the highest CA is shown in Figure 4(b) with 600 mm/min and 1.2 W. Additionally, each scan speed corresponds to the highest recorded CA value at 1.2 W laser power.

3.2 Morphology Analysis

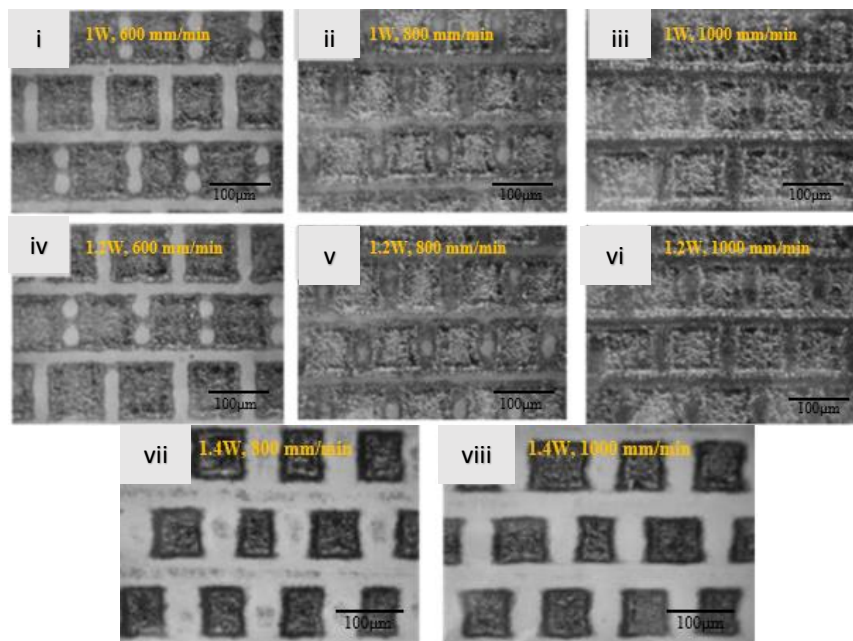
Figures 5(a) and 5(b) illustrate the morphologies of the glass surface, (i), (ii), and (iii) experienced laser power at 1.0W, (iv), (v), (vi) experienced laser power at 1.2W and (vii), and (viii) experienced laser power at 1.4W with scanning speed increasing at 600, 800 and 1000 mm/min respectively for a pattern with hatch spacing 0.3 and 0.5 mm.

Figure 5(a) shows how the laser treatment resulted in a homogeneous coating of micro/nanoparticles of various sizes on the initially smooth surface between the bricklayer scan lines [18]. All the fabricated samples have different finishing in terms of the size of the pattern design, this occurs because of the different parameters used. Figures (i), (ii), (iii), and (vi) show the pattern, although it hardly resembles the one intended because there was a mass of particles surrounding them and the micro/nanostructures of surfaces were more enriched than in (iv) and (v).

Pulsed laser ablation for micro/nanostructures has grown popular due to its efficiency and precision. A heat-affected zone (HAZ) develops when a substrate is subjected to laser radiation because the surface material absorbs the energy. Although the surface temperature rises when exposed to laser light, no discernible morphological change occurs [18][19].



(a)



(b)

Figure 5. Micrograph of the modified glass by different laser process parameters for (a) 0.3 mm spacing pattern, (b) 0.5 mm spacing pattern

A crack appears for this sample and results from samples (i) to (vi) in Figure 5(b) are comparable and reliable in terms of pattern size compared to 0.3 mm patterns. The samples (vii) and (viii) display outstanding results with no sample cracks. The thermal stress brought on by the process' rapid heating and cooling is reported to induce cracks to form in the scanning direction. It is found that as the laser power and scan speed increase, more laser energy is deposited on the glass, which causes the crack's size to enlarge. The size of the cracks produced varies depending on the process settings from a few tens of microns to a few hundreds of microns [20].

Both sample patterns with 0.3 and 0.5 mm spacing show no defect, and all the samples have a mark from the laser textures. With an increase in power, the laser marks on the surface become wider, and the gap between the lines becomes more distinct. However, as the scanning speed increases, the gap between the marked lines decreases, and the lines become less defined. The laser beam's smooth morphology may be seen on the glass surface it has illuminated. This shows that there is no material loss and that the laser beam's interaction with the glass solely causes volume melting below the surface [20].

4. Conclusion

In conclusion, our research has shown how easily flat soda-lime glass surfaces' wettability can be altered through the diode laser processing solution and measurement of water contact angle using a sessile drop test. According to our findings, the surface can change from hydrophilic to hydrophobic with contact angles ranging from 32.25° to nearly 98.97° , emphasizing surface morphology's essential importance in determining crack propagation. After laser processing, the water contact angle significantly improves to 64.14° , representing a substantial increase of 30° compared to the unmodified glass. During surface modification, the effects of laser power and scan speed were examined. Upon observing the micrographs of the modified glass surface, visible line cracks were observed, and the sample displayed line marks with increased spacing between the lines as the scanning speed decreased. With surface textures, the current work deepens our understanding of glass surface hydrophobicity. With the help of laser texture parameters, it provides a stable framework for adjusting the hydrophobicity of soda-lime glass surfaces.

Declaration of competing interest

The authors claim that none of their known financial or interpersonal disputes could have possibly impacted the findings presented in this study.

Acknowledgment

The authors would like to express their gratitude for the financial assistance provided by the Ministry of Higher Education Malaysia under the FRGS/1/2021/TK0/UMP/02/48. (UMP grant no: RDU210145) for funding this research.

References

- [1] T. H. Dinh, C. V. Ngo, and D. M. Chun, "Direct laser patterning for transparent superhydrophobic glass surfaces without any chemical coatings," *Appl. Phys. A Mater. Sci. Process.*, vol. 126, no. 6, pp. 1–11, 2020, doi: 10.1007/s00339-020-03653-9.
- [2] V. Kumar, R. Verma, V. Sharma, and S. Kango, "Recent progresses and applications in Laser-based surface texturing systems," *Mater. Today Commun.*, vol. 26, Oct. 2020, doi: 10.1016/J.MTCOMM.2020.101736.
- [3] J. Chao, J. Feng, F. Chen, B. Wang, Y. Tian, and D. Zhang, "Fabrication of superamphiphobic surfaces with controllable oil adhesion in air," *Colloids Surfaces A Physicochem. Eng. Asp.*, vol. 610, no. September 2020, p. 125708, 2021, doi: 10.1016/j.colsurfa.2020.125708.
- [4] K. Yin, Z. Wu, J. Wu, Z. Zhu, F. Zhang, and J.-A. Duan, "Solar-driven thermal-wind synergistic effect on laser-textured superhydrophilic copper foam architectures for ultrahigh efficient vapor generation," *Appl. Phys. Lett.*, vol. 118, no. 21, p. 211905, May 2021, doi: 10.1063/5.0050623.
- [5] Q. Wang, Y. Cheng, Z. Zhu, N. Xiang, and H. Wang, "Modulation and control of wettability and hardness of zr-based metallic glass via facile laser surface texturing," *Micromachines*, vol. 12, no. 11, 2021, doi: 10.3390/mi12111322.
- [6] Y. Liu *et al.*, "An experimental study to characterize a surface treated with a novel laser surface texturing technique: Water repellency and reduced ice adhesion," *Surf. Coatings Technol.*, vol. 374, no. March, pp. 634–644, 2019, doi: 10.1016/j.surfcoat.2019.06.046.
- [7] H. Wang, J. Zhuang, H. Qi, J. Yu, Z. Guo, and Y. Ma, "Laser-chemical treated superhydrophobic surface as a barrier to marine atmospheric corrosion," *Surf. Coatings Technol.*, vol. 401, no. July, p. 126255, 2020, doi: 10.1016/j.surfcoat.2020.126255.
- [8] K. Indira, C. Sylvie, W. Zhongke, and Z. Hongyu, "Investigation of Wettability Properties of Laser Surface Modified Rare Earth Mg Alloy," *Procedia Eng.*, vol. 141, pp. 63–69, 2016, doi: 10.1016/j.proeng.2015.08.1106.
- [9] M. S. Ahsan, F. Dewanda, M. S. Lee, H. Sekita, and T. Sumiyoshi, "Formation of superhydrophobic soda-lime glass surface using femtosecond laser pulses," *Appl. Surf. Sci.*, vol. 265, pp. 784–789, 2013, doi: 10.1016/j.apsusc.2012.11.112.
- [10] T.-H. Dinh, C. V. Ngo, and D.-M. Chun, "Direct laser patterning for transparent superhydrophobic glass surfaces without any chemical coatings," *Appl. Phys. A*, vol. 126, May 2020, doi: 10.1007/s00339-020-03653-9.
- [11] M. Soldera, S. Alamri, P. A. Sürmann, T. Kunze, and A. F. Lasagni, "Microfabrication and surface functionalization of soda lime glass through direct laser interference patterning," *Nanomaterials*, vol. 11, no. 1, pp. 1–17, 2021, doi: 10.3390/nano11010129.
- [12] H. Teisala, M. Tuominen, and J. Kuusipalo, "Superhydrophobic Coatings on Cellulose-Based Materials: Fabrication, Properties, and Applications," *Adv. Mater. Interfaces*, vol. 1, Feb. 2014, doi: 10.1002/admi.201300026.
- [13] A. Ouchene *et al.*, "Roughness and wettability control of soda-lime silica glass surfaces by femtosecond laser texturing and curing environments," *Appl. Surf. Sci.*, vol. 630, no. May, 2023, doi: 10.1016/j.apsusc.2023.157490.

- [14] G. Dongre, A. Rajurkar, R. Raut, and S. Jangam, "Preparation of super-hydrophobic textures by using nanosecond pulsed laser," *Mater. Today Proc.*, vol. 42, no. January, pp. 1145–1151, 2020, doi: 10.1016/j.matpr.2020.12.497.
- [15] ASTM D7490, "ASTM D7490: Measurement of the Surface Tension of Solid Coatings, Substrates and Pigments using Contact Angle Measurements," pp. 1–5, 2013, doi: 10.1520/D7490-13.2.
- [16] R. Coatings, "Standard Practice for Surface Wettability of Coatings , Substrates and Pigments by Advancing Contact Angle Measurement 1," *Annu. B. ASTM Stand.*, vol. i, no. C, pp. 8–10, 2011, doi: 10.1520/D7334-08R13.2.
- [17] Z. Song, F. Guo, Y. Liu, S. Hu, X. Liu, and Y. Wang, "Controllable bidirectional wettability transition of impregnated graphite by laser treatment and transition mechanism analysis," *Surf. Coatings Technol.*, vol. 317, pp. 95–102, 2017, doi: 10.1016/j.surfcoat.2017.03.047.
- [18] R. Zhou, F. Shen, J. Cui, Y. Zhang, and H. Yan, "Electrophoretic Deposition of Graphene Oxide on Laser-Ablated Copper Mesh for Enhanced Oil / Water Separation," 2019, doi: 10.3390/coatings9030157.
- [19] Y. Reg, C. Kägeler, and M. Schmidt, "Experimental studies on effects at micro-structuring of highly reflecting metals using nano- and picosecond-lasers," *Phys. Procedia*, vol. 5, pp. 245–253, 2010, doi: 10.1016/j.phpro.2010.08.143.
- [20] J. Shin, "applied sciences Groove Formation in Glass Substrate by a UV Nanosecond Laser," 2020.